Short focal length Kirkpatrick-Baez mirrors for a hard x-ray nanoprobe

Wenjun Liu
Oak Ridge National Laboratory, Oak Ridge, Tennessee 37831 and University of Illinois at Urbana-Champaign, Urbana, Illinois 61801

Gene E. Ice and Jonathan Z. Tischler
Oak Ridge National Laboratory, Oak Ridge, Tennessee 37831

Ali Khounsary, Chian Liu, Lahsen Assoufid, and Albert T. Macrander
Argonne National Laboratory, Argonne, Illinois 60439

(Received 10 August 2005; accepted 19 September 2005; published online 7 November 2005)

We describe progress in the fabrication of short-focal-length total-external-reflection Kirkpatrick-Baez x-ray mirrors with ultralow figure errors. The short focal length optics produce nanoscale beams (<100 nm) on conventional (~64 m long) beamlines at third generation synchrotron sources. The total-external reflection optics are inherently achromatic and efficiently focus a white (polychromatic) or a tunable monochromatic spectrum of x rays. The ability to focus independent of wavelength allows novel new experimental capabilities. Mirrors have been fabricated both by computer assisted profiling (differential polishing) and by profile coating (coating through a mask onto ultra-smooth surfaces). A doubly focused 85×95 nm^2 hard x-ray nanobeam has been obtained on the UNICAT beamline 34-ID at the Advanced Photon Source. The performance of the mirrors, techniques for characterizing the spot size, and factors limiting focusing performance are discussed. © *2005 American Institute of Physics.* [DOI: 10.1063/1.2125730]

I. INTRODUCTION

Essential to the study of nanophase materials is an understanding of elemental composition, crystal structure, local bonding states, and defects. X-ray diffraction and spectroscopy are widely used to probe these properties, and the availability of high-brilliance third-generation and the commissioning of new fourth-generation synchrotron sources has stimulated an emergence of interest in x-ray micro/nanofocusing optics.[1–3] Whereas the development of advanced x-ray optics now allows for routine hard x-ray experiments with submicron resolution,[4,5] even smaller x-ray beams are needed to study nanophase materials on the natural length scale of individual nanoparticles.

Various methods have been proposed to produce small focused x-ray beams and efforts currently underway include Fresnel Zone plates,[2] Kirkpatrick-Baez (K-B) mirrors,[1,6–9] compound refractive lenses,[10] Bragg-Fresnel optics,[11] and tapered capillaries.[12] Total external specular-reflecting K-B mirrors are particularly attractive for micro/nanofocusing broad bandpass x-ray beams or for use with tunable beams, since they are inherently nondispersive. Nondispersive optics greatly-simplify experiments on individual nanoparticles. In particular, the difficulties associated with rotations of nanoscale samples are avoided because spectroscopies and diffraction based on scanned monochromatic beams can provide reliable nanoscale information about the sample coordination, chemistry and structure while the sample orientation and position remains fixed during the measurement.

In the Kirkpatrick-Baez geometry, two glancing-angle concave mirrors collect and focus x rays in alternate planes.[13] The major challenge to achieve micro or nanofocused x-ray beams, is the need to fabricate ultrasmooth elliptical surfaces with submicroradian figure errors. For sub-100 nm level focusing K-B mirrors, figure perfection below a few tenths of microradians and surface roughness less than a few angstroms are essential.

In this article, we describe new developments in the fabrication of short-focal-length K-B mirrors with ultralow figure errors. Mirrors have been produced by computer aided profiling (differential polishing) and by profile coating techniques, respectively. A doubly focused 85×95 nm^2 monochromatic nanobeam at 15 keV has been obtained on a standard length beamline at the Advanced Photon Source. An even smaller (~80 nm) horizontal focus was measured for a polychromatic beam with x rays from ~7 to 22 keV. The beamline layout, performance of the mirrors, techniques for characterizing the spot size, and factors limiting performance are discussed.

II. BEAMLNE CONFIGURATIONS

A prototype hard x-ray nanofocusing system has been developed and tested at the 34-ID-E station of the APS. The source is an APS type A undulator with source parameters described previously.[14] Figure 1 schematically illustrates the beamline layout of 34-ID and the nanoprobe setup. The experimental station is located about 64 m from the source. Slits can be used to relax the required geometrical demagnification when image size is more important than flux. For example, a slit at 28 m was placed to control the total power in the beam and to reduce the undulator horizontal source size of ~700 μm down to <100 μm; thus it also acts as a

 © 2005 American Institute of Physics

Downloaded 04 Sep 2009 to 160.91.157.167. Redistribution subject to AIP license or copyright; see http://rsi.aip.org/rsi/copyright.jsp

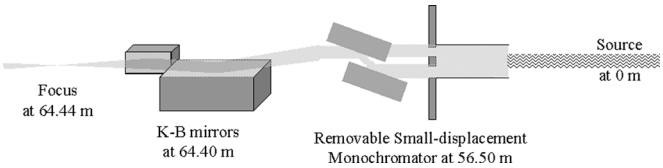

FIG. 1. A prototype hard x-ray K-B nanofocusing system at the 34-ID-E station of the APS. The beam can be rapidly switched between monochromatic and polychromatic modes.

new effective object. In the vertical plane, the undulator source, with FWHM of about 40 μm serves directly as the object.

A 40 mm long primary mirror with focal length of 60 mm for focusing in the vertical plane and a 20 mm long secondary mirror with focal length of 30 mm for focusing in the horizontal (ring) plane are combined to achieve sub-100 nm x-ray beam. The mirror optics have demagnifications of about 1200:1 horizontally and 1100:1 vertically.

On beamline 34-ID, a special small-displacement Si(111) double-crystal monochromator allows the energy bandpass to be rapidly changed between monochromatic beams ($\Delta E/E \sim 2\times 10^{-4}$) and polychromatic beams ($\Delta E/E \sim 1$). The monochromator displaces the x-ray beam by about 1 mm but is designed to take the beam to be monochromated from a lower portion of the incident beam, so that the monochromatic and polychromatic x-ray beams can pass through the same exit slit.[15] Although the monochromatic and polychromatic beams exit the same slit, the vertical displacement of monochromatic beam results in a small angular change of about 20 μrad, which displaces the monochromatic focus from polychromatic focus by ~ 1 μm vertically. This angular displacement can be corrected by heating the second crystal to slightly increase the d spacing and thus to tilt the monochromatic beam, so that the monochromatic beam is parallel and coincident to the polychromatic beam. The monochromator also uses flex pivot rotations to reduce slip and stiction, and can be turned over a wide energy range of about 7–22 keV.

Table I lists all the key optical parameters of our nanofocusing system. With high reflectivity of the mirrors, the gain is estimated to be about 10^5.

III. MIRROR FABRICATION AND METROLOGY

In the 34-ID nanofocusing mirror system, two different technologies were used to produce the elliptical mirrors. One mirror was fabricated (i.e., elliptically figured) by a computer-aided differential polishing method, while the other mirror was made by profile coating on an ultraflat substrate. Both techniques produce monolithic optics that is inherently more stable and more compact than dynamically bent mirror optics.

TABLE I. Optical parameters of the K-B nanofocusing mirrors.

Parameters	Vertical mirror	Horizontal mirror
Fabrication method	Polishing	Deposition
Surface coating material	Pd	Au
Mirror length	40 mm	20 mm
Focal length	60 mm	30 mm
Geometrical demagnification	1100	1200
Mirror glancing angle	3 mrad	3 mrad
Maximum beam acceptance	120 μm	60 μm

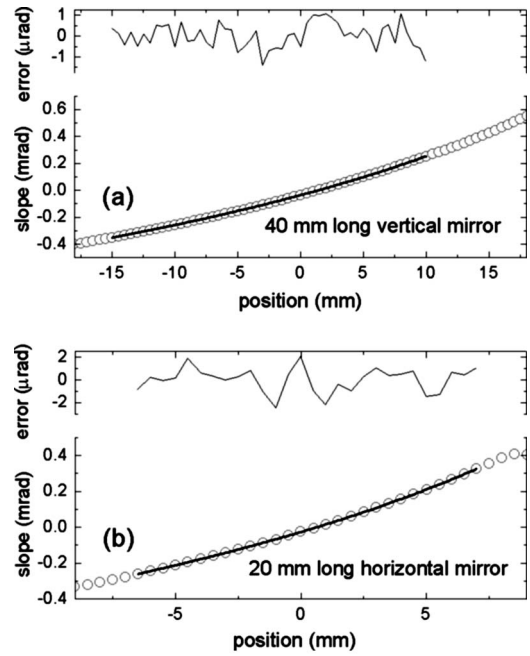

FIG. 2. Mirror figures measured by LTP. The rms deviation from the ideal ellipse can be even less over smaller regions of the mirror when ignoring the both ends. (a) Vertical mirror; (b) horizontal mirror.

A. Vertical mirror

The vertical focusing 40 mm long mirror was fabricated by Tinsley Laboratories Incorporated using their Computer Controlled Optical Surfacing (CCOS) technique (a differential polishing method).[16] Tinsley Laboratories pioneered the use computer controlled optical surfacing to produce state-of-the-art computer-generated nonspherical surfaces for lithographic optics. Float-zone single-crystal silicon was used as the substrate for making the vertical mirrors. The substrate was etched and evaluated for possible residual stress before polishing. Stress relief cuts were made to allow for polishing on a large surface with the smaller mirror surfaces contiguous with the overall large polished surface.

State-of-the-art metrology is required to measure and correct figure perfection with slope errors on the order of tenths of a microradian. Slope errors are particularly serious for nanofocusing with the primary KB mirror that has twice the focal length of the secondary mirror. In order to measure slope errors on the order of 0.1 μrad, measurement system accurate to 0.1 nm height over spatial wavelength of 0.5 mm are needed. During the fabrication, a precise Fizeau interferometer with a specially made compensating lens was used to check the figure. Before the mirror was installed on the beamline, independent interferometric measurements were made that verified the mirror figure and figure errors. In addition, long-trace profiler (LTP) measurements were also performed at the APS metrology laboratory to assess the mirror quality before and after it was uniformly coated with Pd for higher reflectivity in the desired energy range.[17] Figure 2(a)

Downloaded 04 Sep 2009 to 160.91.157.167. Redistribution subject to AIP license or copyright; see http://rsi.aip.org/rsi/copyright.jsp

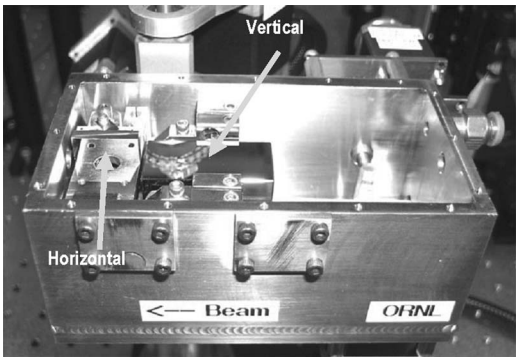

FIG. 3. Nanoprobe mirror tank. The white arrows indicate vertical and horizontal mirrors.

is a comparison of the ideal and actual figure for an elliptical surface of the vertical mirror. The measured root-mean-square (RMS) slope errors are in the 0.4–0.6 μrad range.

B. Horizontal mirror

The 20 mm long horizontally focusing mirror was produced by profile coating at the APS deposition laboratory.[18] This technique passes the substrate in a dc magnetron sputtering system over a contoured mask to deposit a predetermined depth profile onto a flat substrate. The shape of the contour is calculated according to the desired elliptical profile of an ideal final mirror and from the measured shape of the original substrate surface. In principle, any substrate figure can be used. As flat Si substrates with excellent smoothness and flatness are commercially available and inexpensive, these are currently the substrate of choice.

The use of profile coating overcomes many of the difficulties of polishing asymmetrical mirror surfaces and provides the x-ray community with a practical way of obtaining high-performance monolithic K-B mirrors for micro/nanofocusing. Profile coating is also reproducible and allows for the fabrication of many similar mirrors. Profile coating thus has tremendous technical and fiscal advantages for the synchrotron community.

Figure 2(b) shows a typical LTP result demonstrating that a flat Si substrate can be converted into an elliptical one with a single profile coating. The coating profile is obtained from the difference between the measured profile of the substrate and the profile of a perfect ellipse. The profile coating does not deteriorate the surface roughness of the substrate, when the coating material was gold with 5 nm thick Cr as an adhesion layer.

IV. MIRROR PERFORMANCE AND ALIGNMENT TOLERANCES

Until recently, geometrical demagnification and figure errors have been the major limitations to x-ray resolution with Kirkpatrick-Baez mirrors. However as mirror quality improves, alignment and vibration become serious challenges that ultimately must be minimized to reach the diffraction limit. We have developed a very compact mirror box, shown in Fig. 3, to hold and align the two sequential K-B mirrors. Vibration is minimized through the use of stiff low-mass components. In addition, the short focal length optics contributes to a strong geometrical demagnification, and also minimizes the influence of vibration.[19]

For an ideal elliptical focusing mirror, locally the radius of mirror curvature is given by

$$R = \frac{2f_1 f_2}{(f_1 + f_2)\sin\theta}. \tag{1}$$

Here f_1 is the object distance, f_2 is the image distance, and θ is the mirror angle. In a real mirror, variations from an ideal surface blur the beam focus. For example, short period surface roughness can cause diffuse x-ray scattering that reduces the focused beam intensity and contributes to background. The total intensity of a geometrically demagnified beam is approximated by

$$I = I_0 \exp\left[-\left(\frac{4\pi\theta\sigma_s}{\lambda}\right)^2\right], \tag{2}$$

where σ_s is the rms surface roughness of spatial frequencies below $\sim$1 cm and λ is the x-ray wavelength.[1] For 90% power into the geometrical image, a typical operational energy of 15 keV at 3 mrad glancing angle requires $\sigma_s < 0.7$ nm. With modern polishing and deposition techniques, surface roughness is typically not a serious problem for nanoprobe optics.

However, surface figure and focal aberrations remain as important barriers to achieve diffraction-limited focusing optics. Long-period deviations from an ideal mirror surface are referred to as figure errors. The figure error blurring of the image can be estimated from the rms figure deviation from an ideal elliptical surface, σ_f, and from the focal length f_2. Because reflected rays deviate by twice the angular error of the surface profile, and assuming a Gaussian distribution of errors where the full-width-half-maximum, FWHM, is 2.35σ, then the FWHM blurring S_f due to slope errors is,

$$S_f \approx 4.7\sigma_f f_2. \tag{3}$$

It is clear that longer focal length results in larger blurring for a given surface perfection. With a 30 mm focal length, a figure error of 0.2 μrad will have blurring of about 30 nm. It is therefore useful to produce low figure error elliptical surface with small focal lengths. Unfortunately it is often harder to fabricate a short mirror with ultralow figure errors than to make an intermediate length mirror with the same figure errors.[20]

K-B mirror focusing has been studied extensively by using ray-tracing methods.[1] However when diffraction-limited mirrors can be procured, numerical wave optical simulations are needed to understanding the interaction of mirror length, source size and intermediate apertures to focal size.[21] The diffraction-limited focal spot size at FWHM can be estimated by

$$S_d \approx \frac{0.88 f_2 \lambda}{d} \tag{4}$$

for a rectangular aperture.[22] d is the aperture size determined by mirror length and angle. At 3 mrad glancing angle and with a length of 40 mm, the acceptance of the vertical mirror is 120 μm. The acceptance of the horizontal mirror is

Downloaded 04 Sep 2009 to 160.91.157.167. Redistribution subject to AIP license or copyright; see http://rsi.aip.org/rsi/copyright.jsp

60 μm. At 15 keV, our nanofocusing optics has a theoretical diffraction limit of about 40 nm in both horizontal and vertical directions. Since the mirror fabrication is not yet precise enough over the entire mirror, a rectangular acceptance aperture is placed before the mirror box to select a fraction of the mirror surfaces for best focusing performance. Of course this method of reducing beam blurring from figure errors increases the diffraction limit and limits the available flux. The estimated gain into a sub 100 nm spot is $\sim 10^5$ with mirror reflectivity of $>70\%$ at 15 keV. We note that with better mirrors, the full mirror surface can be used which collects more x rays into a smaller spot. The estimated gain from ideal mirrors will be $\sim 1.6\times 10^6$.

Careful alignment is required to achieve a focused beam with sub-100 nm resolution in both directions. For example, the mirror glancing angles, alignment of the perpendicularity of the mirror pair, and alignment of the mirror in-plane rotations are all important. Our simulation and measurement showed that at ~ 3 mrad glancing angle, 2 μrad rotations can cause observable peak broadening ($>5\%$) from the ideal focal size. Nonperpendicularity of two mirrors will also induce severe blurring on the focus. To focus a 100×100 μm^2 incident beam down to a 100×100 nm^2, the misalignment of two mirror glancing angle axes must be <1 mrad. Our mirror box provides about 0.2 mrad precision of mirror perpendicularity with the aid of optical laser levels. In addition, the effect of mirror in-plane rotation needs to be considered, but the acceptable tolerance of angular error of about a few degrees is easy to be guaranteed.

Our nanofocusing system has a depth-of-field of about 100 μm, which is sufficient for many samples in terms of x-ray penetration depth. However, to keep vertical and horizontal foci at a same point during the experiment, the vibration and thermal drifting of the mirror system must also be minimized.

V. MEASUREMENT OF FOCAL SIZE

Several techniques have been used to evaluate the focal spot size of x-ray micro and nanobeams. Pt or Au wire absorption scans and knife-edge fluorescence scans are the most common ways to characterize the focal spot properties.[1,2] However, to measure a sub-100 nm sized x-ray beam, the derivative nature of the wire scan or knife-edge methods requires high linearity of the translation mechanism; the translation must be controlled within a few nanometers with high demand on signal-to-noise ratio. We therefore developed a nanoslit/reflector to precisely characterize the beam profile, shown in Fig. 4(a). In addition, to accelerate the tedious process of mirror alignment, a patterned Au stripe mask having equally 200 μm spaced multiple nanoslits/reflectors was used, as illustrated in Fig. 4(b).

The nanoslit/reflector was fabricated by e-beam lithography. A 5 μm wide and 10 nm thick Au stripe was deposited on a flat Si substrate. When measuring the focal spot, the Au stripe was scanned across the beam at glancing angle of <4 mrad. Either Au fluorescence or the reflected intensity by Au film can be collected; thus the Au stripe is equivalent to a ~ 20 nm wide pseudoslit or reflector. In a real measurement, the patterned multiple nanoslits/reflectors can profile the beam at every 200 μm along the beam axis, so that the focal point can be quickly located and precisely measured.

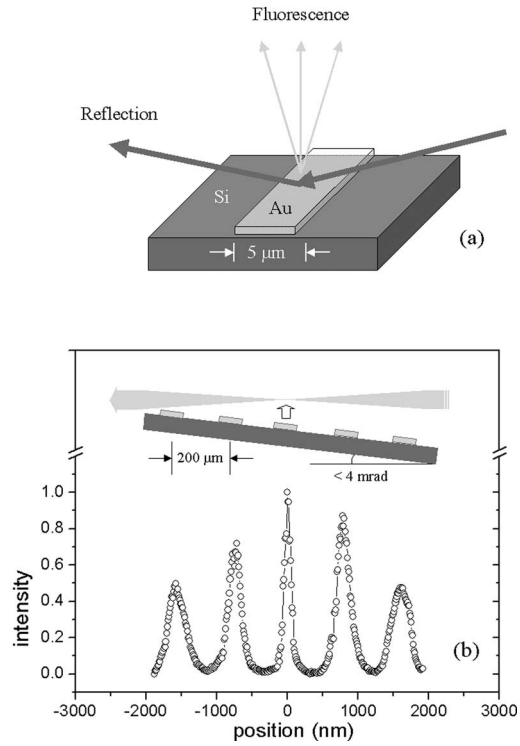

FIG. 4. Patterned gold mask for precise and fast characterization of the beam profile. Either Au fluorescence or the reflected intensity by Au film can be collected. (a) A single Au stripe at glancing angle is equivalent to a ~ 20 nm wide pseudoslit or reflector. (b) Multiple nanoslits/reflectors were scanned across the beam at every 200 μm along the beam axis.

Our prototype x-ray nanofocusing system based on differentially polished and profile-coated mirrors has been installed and tested. As shown in Fig. 5, a doubly focused 85×95 nm^2 monochromatic nanobeam at 15 keV was achieved. Both measured horizontal and vertical focal sizes are bigger than the geometrically demagnifications and the diffraction limits. This indicates that mirror imperfection and vibrations of the optical system are major contributions to focus blurring.

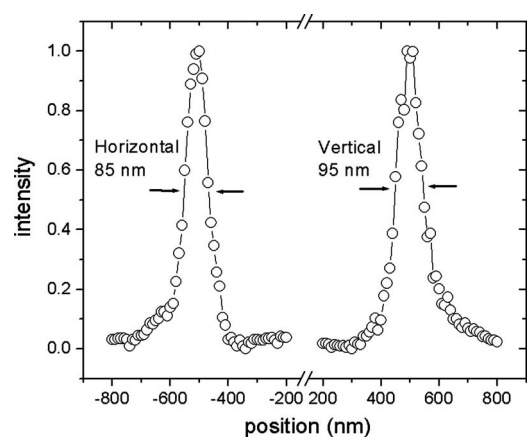

FIG. 5. Doubly focused 85×95 nm^2 monochromatic nanobeam at 15 keV. The intensity profiles were obtained by scanning a Au nanoslit/reflector across the beam.

Downloaded 04 Sep 2009 to 160.91.157.167. Redistribution subject to AIP license or copyright; see http://rsi.aip.org/rsi/copyright.jsp

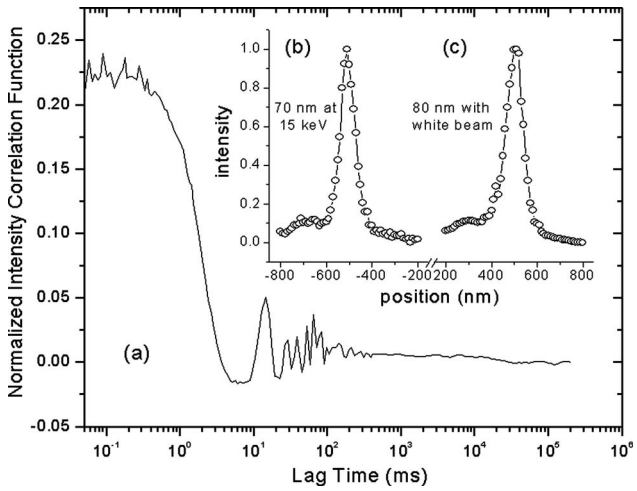

FIG. 6. Vertical vibration spectrum measured by fluorescence correlation function spectroscopy. (a) The amplitude of vibration is on the order of 70–80 nm at dominated frequency of 63±5 Hz. (b) and (c) Smaller focal spot sizes obtained in horizontal by turning off power to the most likely vibration sources.

Fluorescence correlation spectroscopy was used to analyze the vibration spectrum of the system.[23] Figure 6(a) is a typical fluorescence correlation function spectrum. The measured vibration was on the order of 70–80 nm at a dominated frequency of 63±5 Hz. By turning off power to the most likely vibration sources, the focal spot size was found to be sometimes significantly smaller. A horizontal focus of approximately 70 nm was measured at 15 keV, while the white beam focus under the same conditions was about 80 nm, as shown in Figs. 6(b) and 6(c).

VI. DISCUSSION

In general, perfect elliptical mirrors can focus small sources to images that are very close to their geometrical and diffraction limits. Real optics however can have significant deviations. Besides limiting factors discussed earlier, windows and other scattering sources can also degrade the focusing performance by shortening the object distance and by increasing the effective object size. The number of windows should therefore be restricted, and they should be polished to minimize scattering. The measurements reported in this article were performed with a standard APS graphic thermal filter associated with a so-called commissioning window. It is anticipated that focal size and efficiency can be improved by removing this window.

The limit of our current nanofocusing optics is set by diffraction, although ultimately blurring due to x-ray beam penetration into the reflecting surface will be a concern. Total-external-reflection mirrors have a shallow evanescent wave penetrating into the mirror surface, which smears the reflected beam. For a Pd coated mirror at 3 mrad glancing angle, the blur introduced by beam penetration is less than 5 nm, which is negligible now.

Assuming that 40 nm diffraction-limited mirrors can be procured as the mirror figuring and smoothness technologies mature, one way to further reduce the beam size is by stacking two identical K-B mirrors, as illustrated in Fig. 7. The geometry allows for a short focal length in both horizontal and vertical directions to reduce the demand for low figure error, and a slightly larger solid angle can be accepted which allows for smaller diffraction limited focusing. Although side-by-side mirrors offer an attractive approach that simplifies the nanoprobe focusing optics, there are serious technical challenges to use such mirrors: (1) an ultrasmooth mirror must be cut without distortions; and (2) damage extending more than a few microns from the mirror intersection can seriously degrade the focusing performance and efficiency due to loss of useful mirror reflecting surface.

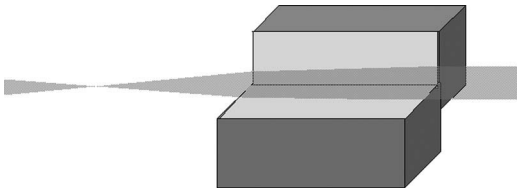

FIG. 7. Schematic of side-by-side Kirkpatrick-Baez mirrors. Both vertical and horizontal mirrors have identical figures and focal lengths.

In summary, Kirkpatrick-Baez optics are particularly promising elements for nondispersive nanofocusing of hard x rays over a wide bandpass. Although the results obtained so far are still far from optimized as a truly nanoscale x-ray probe, the sub-100 nm focusing already provides immediate opportunities for first-of-a-kind characterizations of nanomaterials and high spatial resolution investigation of materials microstructure and evolution.

ACKNOWLEDGMENTS

Research sponsored by the U.S. Department of Energy under Contract No. DE-AC05-00OR22725. The UNICAT facility at the APS is supported by the U.S. DOE under Award No. DEFG02-91ER45439. The authors thank Bennett C. Larson, Paul Zschack, Wenge Yang, Ralu Divan, Yujie Wang, Ray Conley, Jun Qian, Kristina Young, Derrick Mancini, and Jörg Maser for their help during this work.

[1] G. E. Ice, J.-S. Chung, J. Z. Tischler, A. Lunt, and L. Assoufid, Rev. Sci. Instrum. **71**, 2635 (2000).
[2] W. Yun, B. Lai, Z. Cai, J. Maser, D. Legnini, E. Gluskin, Z. chen, A. A. Krasnoperova, Y. Vladimirsky, F. Cerrina, E. di Fabrizio, and M. Gentili, Rev. Sci. Instrum. **70**, 2238 (1999).
[3] A. Freund, J. Phys. IV **104**, 165 (2003).
[4] B. C. Larson, W. Yang, G. E. Ice, J. D. Budai, and J. Z. Tischler, Nature (London) **415**, 887 (2002).
[5] W. Liu, G. E. Ice, B. C. Larson, W. Yang, J. Z. Tizchler, and J. D. Budai, Metall. Mater. Trans. A **35**, 1963 (2004).
[6] O. Hignette, P. Cloetens, W.-K. Lee, W. Ludwig, and G. Rostaing, J. Phys. IV **104**, 231 (2003).
[7] K. Yamamura, K. Yamauchi, H. Mimura, Y. Sano, A. Saito, K. Endo, A. Souvorov, M. Yabashi, K. Tamasaku, T. Ishikawa, and Y. Mori, Rev. Sci. Instrum. **74**, 4549 (2003).
[8] O. Hignette, P. Cloetens, G. Rostaing, P. Bernard, and C. Morawe, Rev. Sci. Instrum. **76**, 063709 (2005).
[9] H. Yumoto, H. Mimura, S. Matsuyama, H. Hara, K. Yamamura, Y. Sano, K. Ueno, K. Endo, Y. Mori, M. Yabashi, Y. Nishino, K. Tamasaku, T. Ishikawa, and K. Yamauchi, Rev. Sci. Instrum. **76**, 063708 (2005).
[10] A. Snigirev, V. Kohn, I. Snigireva, and B. Lengeler, Nature (London) **384**, 49 (1996).
[11] M. Yasa, Y. Li, C. B. Mammen, J. Als-Nielsen, J. Hoszowska, C. Mocuta, and A. Freund, Appl. Phys. Lett. **84**, 4744 (2004).
[12] D. H. Bilderback, X-Ray Spectrom. **32**, 195 (2003).

Downloaded 04 Sep 2009 to 160.91.157.167. Redistribution subject to AIP license or copyright; see http://rsi.aip.org/rsi/copyright.jsp

[13] P. Kirkpatrick and V. Baez, J. Opt. Soc. Am. **38**, 766 (1948).
[14] Advanced Photon Source Annual Report (2004).
[15] G. E. Ice, J.-S. Chung, W. Lowe, E. Williams, and J. Edelman, Rev. Sci. Instrum. **71**, 2001 (2000).
[16] http://www.asphere.com
[17] L. Assoufid, A. Khounsary, J. Qian, A. T. Macrander, and D. Mills, Proc. SPIE **4501**, 54 (2001).
[18] C. Liu, L. Assoufid, R. Conley, A. T. Macrander, G. E. Ice, and J. Z. Tischler, Opt. Eng. **42**, 3622 (2003).
[19] G. E. Ice, E. D. Specht, J. Z. Tischler, A. Khounsary, L. Assoufid, and C. Liu, Proc. SPIE **5347**, 1 (2003).
[20] Andy Lunt, Tinsley Laboratories, Richmond, CA (private communication).
[21] Y. Mori, K. Yamauchi, K. Yamamura, H. Mimura, Y. Sano, A. Saito, K. Ueno, K. Endo, A. Souvorov, M. Yabashi, K. Tamasaku, and T. Ishikawa, Proc. SPIE **4782**, 58 (2002).
[22] M. Born and E. Wolf, *Principles of Optics*, 7th ed. (Cambridge University Press, Cambridge, 1999).
[23] J. Wang, A. K. Sood, P. V. Satyam, Y. Feng, X. Wu, Z. Cai, W. Yun, and S. K. Sinha, Phys. Rev. Lett. **80**, 1110 (1998).

Downloaded 04 Sep 2009 to 160.91.157.167. Redistribution subject to AIP license or copyright; see http://rsi.aip.org/rsi/copyright.jsp